A Rate-Based Model for the Design of Gas Absorbers for the Removal of CO_2 and H_2S Using Aqueous Solutions of MEA and DEA [1]

Nadhir A. Al-Baghli [2], Steven A. Pruess [3], Victor F. Yesavage [4,5], M. Sami Selim [4,5]

---

1 Paper presented at the Fourteenth Symposium on Thermophysical Properties, June 25-30, 2000, Boulder, Colorado, U.S.A.

2 Ph.D. Student at Colorado School of Mines, Golden, Colorado, 80401, U.S.A.

3 Professor of Mathematics at Colorado School of Mines, Golden, Colorado, 80401, U.S.A.

4 Professor of Chemical Engineering at Colorado School of Mines, Golden, Colorado, 80401, U.S.A.

5 Correspondence regarding this paper should be addressed to vyesavag@mines.edu or sselim@mines.edu .

Abstract

A rate-based model was developed for the design of acid-gas absorbers using aqueous alkanolamine solutions. The model adopts the film theory and assumes that thermodynamic equilibrium among the reacting species exists in the bulk liquid. The diffusion-reaction equations for the reacting species in the liquid film are solved using collocation techniques. Heat effects accompanying diffusion and reaction are accounted for using appropriate heat balances on each tray. The algorithm adopts a plate-by-plate calculation starting at the bottom of the tower. Tray hydraulics was added to the algorithm to ensure proper operation of the tower. The program was developed to handle either monoethanolamine (MEA) or diethanolamine (DEA) as chemical solvents.

Key words: alkanolamines, carbon dioxide, hydrogen sulfide, absorption of acid gases, design of absorption towers

1. Introduction

The removal of carbon dioxide and/or hydrogen sulfide from natural gas and other industrial gases using aqueous solutions of alkanolamines is a very important industrial process. The process has been used commercially since the early thirties [1]. Monoethanolamine (MEA), Diethanolamine (DEA), Methyldiethanolamine (MDEA), Diglycolamine (DGA), and Diisopropanolamine (DIPA) are nowadays the most important alkanolamines used in absorption units for the removal of undesirable acid gases.

Two design approaches are in common use; the equilibrium-based approach and the rate-based approach. The equilibrium-based approach is suitable for nonreactive systems. It assumes a theoretical stage in which the liquid and gas phases attain equilibrium. The performance of this stage is then adjusted by applying a tray efficiency correction factor. For reactive systems, such as amine towers, the rate-based approach is more applicable. It is based on analyzing the mass and heat transfer occurring on an actual tray by considering separate mass and energy balances for each phase. These balances are connected by rate equations across the interface. The mass transfer rate across the interface is usually calculated using either the film theory or the penetration theory. Physical equilibrium is assumed to exist at the gas liquid interface and the bulk liquid solution is assumed to be in a state of chemical equilibrium.

The objective of this work is to present an algorithm based on the rate approach, which can be used to design an acid gas absorption tower using aqueous solutions of MEA or DEA. The algorithm is based on a stage by stage calculation treating each tray as a continuous stirred tank reactor (CSTR). Tray hydraulics for a sieve tray column are

incorporated in the program. The effect of operating variables on the number of gas-liquid contact stages is investigated. The algorithm is essential for process simulation and design of gas treating operations.

2. Model Development

The governing equations can best be presented with the aid of Figure 1. This figure illustrates a typical gas-liquid contacting tray. The film theory [2] is adopted to describe the mass transfer of the solute gases across the interface. The sour gas enters the tray at temperature T_{in}^{g}, molar flow rate V_{in} and composition $\vec{y}_{\text{in}}$. It contacts a liquid, which enters the tray at temperature T_{in}^{l}, molar flow rate L_{in} and composition $\vec{x}_{\text{in}}$. Solute gas i crosses the interface into the liquid phase with a flux $N_{i,z}$. All resistances to mass transfer are assumed to be confined to two thin layers next to the interface; the gas film and the liquid film. The thickness of the gas and liquid films are δ_g and δ_l, respectively. The concentration of any liquid reactant k is designated by $C_{k,\text{blk}}$ in the bulk liquid and $C_k(z)$ in the liquid film. Reactions between the absorbed gas and the liquid reactants are assumed to be complete within the liquid film. This implies that the bulk liquid is in a state of chemical equilibrium. Both the liquid and gas on each tray are assumed to be well mixed. Thus the liquid and the gas leaving a tray have the same temperature and composition as the liquid and the gas on the tray, respectively. For the solute gases, CO_2 and H_2S, physical equilibrium at the interface is expressed by

$$P_{i,\,\text{int}} = H_i C_{i,\,\text{int}} \tag{1}$$

where H_i is Henry's constant , $P_{i,\text{ int}}$ is the interfacial partial pressure, and $C_{i,\text{int}}$ is the interfacial molar concentration of the solute gas i. The flux of the solute gas i satisfies the following relations:

$$N_{i,z} = V_{\text{in}} y_{i,\text{in}} - V_{\text{out}} y_{i,\text{out}} = k_{g,i} a\left(P_{i,\text{ out}} - P_{i,\text{ int}}\right) = k_{l,i}^{o} a E_i \left(C_{i,\text{ int}} - C_{i,\text{ blk}}\right) \tag{2}$$

where $k_{g,i}$ and $k_{l,i}$ are the gas and liquid phase physical mass transfer coefficients of the solute gas i, respectively. The subscript blk refers to the bulk, a is the area of the interface, and E_i is the enhancement factor of the dissolved gas i. The latter is defined as the ratio of the rate of absorption of solute gas i in the presence of chemical reaction to that obtained with physical absorption:

$$E_i = \frac{-D_i \left.\frac{dC_i}{dx}\right|_{x=0} + r_i|_{x=0}}{k_l\left(C_{i,\text{ int}} - C_{i,\text{ blk}}\right)} \tag{3}$$

where D_i is the diffusivity of solute gas i in the liquid and $r_i|_{x=0}$ is the rate of surface reaction at the edge of the liquid film ($z = 0$). This term is zero only for non-instantaneous reactions.

For the CO_2-H_2S-Amine-H_2O system, the following equilibrium reactions occur in the bulk of the liquid:

Water Hydrolysis:

$$2\ H_2O \overset{K_{H_2O}}{\rightleftharpoons} H_3O^+ + OH^- \tag{4}$$

Bicarbonate formation:

$$2\ H_2O + CO_2 \overset{K_{CO_2}}{\rightleftharpoons} H_3O^+ + HCO_3^- \tag{5}$$

Carbonate formation:

$$H_2O + HCO_3^- \overset{K_{HCO_3^-}}{\rightleftharpoons} H_3O^+ + CO_3^{--} \quad (6)$$

Bisulfide formation:

$$H_2O + H_2S \overset{K_{H_2S}}{\rightleftharpoons} H_3O^+ + HS^- \quad (7)$$

Sulfide formation:

$$H_2O + HS^- \overset{K_{HS^-}}{\rightleftharpoons} H_3O^+ + S^{--} \quad (8)$$

Amine protonation:

$$H_2O + RR'NH_2^+ \overset{K_{AmH^+}}{\rightleftharpoons} H_3O^+ + RR'NH \quad (9)$$

Carbamate formation:

$$H_2O + RR'NCO_2^- \overset{K_{AmCO_2^-}}{\rightleftharpoons} HCO_3^- + RR'NH \quad (10)$$

where $R = C_2H_4OH$, $R' = H$ for MEA, and $R = R' = C_2H_4OH$ for DEA. In the present work, the model of Kent-Eisenberg [3] was used to find the concentrations of the various species (molecular and ionic) in the bulk of the liquid.

In the liquid film, except for the dissolved gases CO_2 and H_2S, the amine, the amine carbamate, and the protonated amine, the concentrations of the remaining species are assumed to be equal to their corresponding concentrations in the bulk of the liquid. The important reactions that occur in the liquid film are:

$$RR'NH + H_2S \overset{K'_{Am}}{\rightleftharpoons} HS^- + RR'NH_2^+ \quad (11)$$

$$2\,RR'NH + CO_2 \overset{K_{Am}}{\rightleftharpoons} RR'NCO_2^- + RR'NH_2^+ \quad (12)$$

The first reaction is instantaneous since it involves a proton transfer. The second reaction takes place through a zwitterion intermediate. This approach which is derived from Caplow's work [4] was advanced by Danckwerts [5]. Its rate is given for MEA by:

$$-r_{CO_2} = k_{CO_2} C_{CO_2} C_{RR'NH} - \frac{k_{CO_2}}{K_{Am}} \frac{C_{RR'NH_2^+} C_{RR'NCO_2^-}}{C_{RR'NH}} \quad (13)$$

and for DEA by:

$$-r_{CO_2} = \left\{k_{H_2O} C_{H_2O} + k_{RR'NH} C_{RR'NH}\right\}\left\{C_{CO_2} C_{RR'NH} - \frac{C_{RR'NH_2^+} C_{RR'NCO_2^-}}{K_{Am} C_{RR'NH}}\right\} \qquad (14)$$

The rate constants in the above expressions: k_{CO_2}, k_{RRNH}, and k_{H_2O} were reported as functions of temperature by Glasscock et al. [6]

The enhancement factor can be calculated from the concentration profiles of the dissolved gases in the liquid film. This is achieved by solving the following system of five non-linear differential equations governing diffusion and reaction in the liquid film:

$$\frac{d^2 C_{CO_2}}{dz^2} + \frac{r_{CO_2}}{D_{CO_2}} = 0, \quad \frac{d^2 C_{H_2S}}{dz^2} + \frac{D_{HS^-}}{D_{H_2S}} f_1 = 0, \quad \frac{d^2 C_{RR'NH}}{dz^2} + \frac{2 r_{CO_2}}{D_{RR'NH}} + \frac{D_{HS^-}}{D_{RR'NH}} f_1 = 0$$
$$\frac{d^2 C_{RR'NCO_2^-}}{dz^2} - \frac{r_{CO_2}}{D_{RR'NCO_2^-}} = 0, \quad \frac{d^2 C_{HS^-}}{dz^2} - f_1 = 0 \qquad (15a,b,c,d,e)$$

where

$$f_1 = \frac{2K'_{Am}}{f_2}\left(\frac{dC_{RR'NH}}{dz}\frac{dC_{H_2S}}{dz} - \frac{r_{CO_2} C_{H_2S}}{D_{RR'NH}}\right)$$
$$-\frac{2}{f_2}\left(\frac{dC_{RR'NCO_2^-}}{dz}\frac{dC_{HS^-}}{dz} + \left\{\frac{dC_{H_2S}}{dz}\right\}^2\right) - \frac{r_{CO_2} C_{HS^-}}{f_2 D_{RR'NCO_2^-}} \qquad (16)$$

$$f_2 = \frac{D_{HS^-}}{D_{H_2S}} K'_{Am} C_{RR'NH} + \frac{D_{HS^-}}{D_{RR'NH}} K'_{Am} C_{H_2S} + C_{RR'NCO_2^-} + 2C_{HS^-} + \Delta C_{blk} \qquad (17)$$

$$\Delta C_{blk} = C_{RR'NH_2^+,blk} - C_{RR'NCO_2^-,blk} - C_{HS^-,blk} \qquad (18)$$

$$K'_{Am} = \frac{C_{RR'NH_2^+,blk} C_{HS^-,blk}}{C_{RR'NH,blk} C_{H_2S,blk}} \qquad (19)$$

The boundary conditions are:

At $z = 0$: $$\frac{dC_{\mathrm{RR'NCO_2^-}}}{dz} = 0, \qquad D_{\mathrm{RR'NH}} \frac{dC_{\mathrm{RR'NH}}}{dz} + D_{\mathrm{HS^-}} \frac{dC_{\mathrm{HS^-}}}{dz} = 0 \tag{21a,b}$$

$$V_{\mathrm{in}} y_{\mathrm{CO_2,in}} - V_{\mathrm{out}} y_{\mathrm{CO_2,out}} - E_{\mathrm{CO_2}} a k^o_{l,\mathrm{CO_2}} \left(C_{\mathrm{CO_2}}\Big|_{z=0} - C_{\mathrm{CO_2,blk}} \right) = 0 \tag{21c}$$

$$V_{\mathrm{in}} y_{\mathrm{H_2S,in}} - V_{\mathrm{out}} y_{\mathrm{H_2S,out}} - E_{\mathrm{H_2S}} a k^o_{l,\mathrm{H_2S}} \left(C_{\mathrm{H_2S}}\Big|_{z=0} - C_{\mathrm{H_2S,blk}} \right) = 0 \tag{21d}$$

$$K'_{\mathrm{Am}} C_{\mathrm{RR'NH}} C_{\mathrm{H_2S}} - C_{\mathrm{HS^-}} \left(C_{\mathrm{RR'NCO_2^-}} + C_{\mathrm{HS^-}} + \Delta C_{\mathrm{blk}} \right) = 0 \tag{21e}$$

At $z = \delta_l$: $$C_i = C_{i,\mathrm{blk}} \quad \text{for any species } i \text{ in the film} \tag{22}$$

B-spline collocation was used to solve the above system of equations.

3. Heat Effects

The enthalpy of the gas phase, H^{vap}, and the liquid phase, H^{liq}, are given by:

$$H^{vap} = V \sum_i y_i h_i^{vap} \tag{23}$$

$$H^{liq} = L \sum_i x_i h_i^{liq} \tag{24}$$

where h_i^{vap} and h_i^{liq} are the molar enthalpy of component i in the gas and liquid phases, respectively. These are given by:

$$h_i^{vap} = h_{ref}\left(T_{ref}\right) + \overline{C}_{p,i}\left(T - T_{ref}\right) \tag{25}$$

$$h_i^{liq} = h_i^{vap} - \left(+\Delta h_i^V\right) \quad \text{for the solvents } H_2O, \text{ MEA, and DEA} \tag{26}$$

$$h_i^{liq} = h_i^{vap} - \left(-\Delta h_i^{abs}\right) \quad \text{for dissolved } CO_2 \text{ and } H_2S \tag{27}$$

where h_{ref} is the gas enthalpy at some reference temperature T_{ref}, and $\overline{C}_{p,i}$ is the constant pressure ideal gas mean heat capacity. $\left(+\Delta h_i^V\right)$ and $\left(-\Delta h_i^{abs}\right)$ are the heats of vaporization

and absorption of component i, respectively. The heat of absorption includes the effect of mixing and reaction. Equations (23) to (27) assume ideality and are only applied to the molecular components. The effect of the ionic components on the liquid enthalpy is accounted for in the heat of absorption term.

4. Design Method

In the design of absorption towers, it is usually required to find the number of stages needed to achieve a specified degree of separation or vice versa. In both cases, the conditions of the liquid and gas entering the tower are specified. The tower pressure P is either assumed constant across the entire tower or allowance is made for a small pressure drop per tray.

The tower calculations start by assuming a temperature for the gas leaving the tower. A good starting guess is to set the exit gas temperature equal to the inlet liquid temperature; that is, $T_{\text{out}}^{g} = T_{\text{in}}^{\ell}$. Based on the value of T_{out}^{g}, the temperature of the liquid stream leaving the tower can be determined from an overall mass and energy balances around the tower. This gives both the composition and temperature of the liquid stream leaving the first tray (bottom tray) of the tower. Calculations start at the bottom stage and proceed as follows:

1). Appropriate values for the composition of the gas leaving the first stage are assumed. Moreover, assuming thermal equilibrium, the temperature of the gas leaving the first tray may be taken equal to the exit liquid temperature. The mole fraction of water in the gas phase is obtained from Raoult's law. The stage acid gas bulk partial pressure $P_{i,j,\text{blk}}$ is calculated from:

$$P_{i,j,\text{blk}} = y_{i,j} P \qquad i = \text{CO}_2,\ \text{H}_2\text{S} \qquad j = 1 \tag{28}$$

The flux of the acid gas transferred to the liquid phase, $N_{i,j}$, is given by:

$$N_{i,j} = V_{\text{inert}}\left(Y_{i,j-1} - Y_{i,j}\right)\Big/ a \qquad i = \text{CO}_2,\ \text{H}_2\text{S} \qquad j = 1 \tag{29}$$

where V_{inert} is the molar flow rate of the carrier gas and Y_i is the acid gas mole ratio. Next, our system of differential equations (Equations 15) is solved for the concentration profiles of the acid gases in the liquid film. The enhancement factors of the acid gases are then calculated according to Equation (3). With the enhancement factors available, new values for the fluxes are calculated from:

$$N_i = E_{\text{i}}\ a\ k^{\circ}_{l,\text{i}}\left(C_{\text{i}}\big|_{z=0} - C_{\text{i,blk}}\right) \tag{30}$$

The new values of the fluxes are used to update the outlet gas composition. The procedure is repeated until the change in the outlet gas composition is within a specified tolerance. Finally, mass and energy balances between the streams leaving the first stage and the top of the tower give the inlet liquid temperature and composition to that stage.

2) After replacing j by j+1, the calculations in step (1) are repeated for the next stage until the tower outlet gas composition or the number of stages specified is reached.

3) The previous steps are repeated to update the outlet gas temperature. Convergence is achieved when the change in this temperature is within a specified tolerance.

Tray hydraulics including tower diameter, tray spacing, weir height, and pressure drop were obtained from established correlations [7] and added to the algorithm.

5. Results and Discussion

Representative input conditions for an acid gas absorber are summarized in Table I. These conditions were used in our simulator. A summary of the results for MEA and DEA are given in Table II. As can be seen from this table, the number of stages required to meet

the H_2S specification is less for MEA as compared with DEA. This is primarily due to the higher reactivity of MEA with the acid gases. Figure 2 is a representative plot of the concentration profiles of CO_2, H_2S, and DEA on stage 5 of the DEA absorber. Figures 3 and 4 show the vapor composition profiles for CO_2 and H_2S along the MEA and DEA absorbers, respectively. As can be seen, the concentration of H_2S drops down to almost zero at about stage 16 for MEA as compared to stage 18 for DEA. Figure 5 shows the enhancement factors of CO_2 and H_2S for the DEA absorber. As can be seen the enhancement factor for CO_2 increases mildly as we approach the top of the tower. For H_2S, however, the enhancement factor increases sharply until its concentration drops down to almost zero (stage 18) where it reverses trend and starts decreasing as we approach the top of the tower. The corresponding plots for the acid gas loadings (moles of acid gas/ moles of amine) are shown in Figures 6. The figure again reveals that the H_2S loading reaches an asymptotic value at stage 18. Plots for the component stage efficiency are shown in Figure 7. As the figure illustrates the H_2S efficiency reaches its maximum at stage 18 and drops sharply as we reach the top of the tower. For MEA, although not presented, similar behavior is observed throughout for the enhancement factor, acid gas loadings, and the component stage efficiency. As expected, maximum values for these variables were reached at stage 16. It is important to note that the extreme variation of the enhancement factor with stage number, as illustrated in Figure 5, results from the numerical solution of the governing differential equations, and can not be obtained from simple analytical enhancement factor expressions. Furthermore, the variation of stage efficiency with stage number, as shown in Figure 7, implies that the equilibrium-stage efficiency approach is not valid.

Figure 8 shows the temperature profile of the gas or liquid along the tower. From this profile, it can be noticed that a temperature bulge occurs. This temperature bulge may be explained as follows. As the liquid flows down the tower, it continues to absorb acid gas. This absorption is accompanied by a heat of reaction, which causes the temperature of the liquid to continue to rise. The temperature drop at the bottom of the tower results from the cold gas entering the bottom and contacting the hot liquid flowing downwards. The cold gas absorbs heat from the hot liquid causing its temperature to decrease. This results in a temperature bulge at the bottom of the tower.

The effect of the tower pressure on the outlet composition of the acid gases is shown in Table III. The results in this table indicate that the tower outlet acid gas concentration decreases with increasing pressure. This is due to increased acid gas solubility at higher pressure.

References

[1] A.L. Kohl and R.B. Nielsen, Gas Purification, 5th ed., Gulf Publishing Company, Houston, TX, 1997

[2] W.K. Lewis and W.G. Whitman, Ind. Eng. Chem., 16 (1924) 1215.

[3] R.L. Kent and B. Eisenberg, Hydrocarbon Processing, 55 (2) (1976).87.

[4] M. Caplo, J. Am. Chem. Soc, 90 (1968) 6795.

[5] P.V. Danckwerts, Chem. Eng. Sc., 34 (1979), 443.

[6] D.A. Glasscock, J.E. Critchfield, and G.T. Rochelle, Chem. Engng. Sci., 46 (11) (1991), 2829.

[7] A.P. Economopoulos, Chem. Eng., 85 (1978), 109.

Table I Typical Operating Data of Amine-Acid Gas Absorber

Parameter	Value
Inlet gas flow rate, V_{in} (gmol/sec)	500
Inlet liquid flow rate, L_{in} (gmol/sec)	2.0 $L_{\min}$
Inlet gas temperature, T_{in}^{g} (°C)	25
Inlet liquid temperature, T_{in}^{l} (°C)	40
Inlet gas composition, $y_{i,\text{in}}$ (mol %)	CO_2 : 7, H_2S: 5, CH_4: 88
Inlet liquid loading, (gmol/gmol Amine)	CO_2 : 0.02, H_2S: 0.006
Maximum outlet gas composition (PPM vol.)	H_2S: 10
Amine molarity m (gmol/cm^3)	0.002
Absorber pressure P (bar)	40

Table II Design Results of Amine-Acid Gas Absorber

Parameter	MEA	DEA
Outlet gas flow rate, V_{out} (gmol/sec)	444.6	445.5
Outlet liquid flow rate, L_{out} (gmol/sec)	3074.0	2780.0
Outlet gas temperature, T_{out}^{g} (°C)	40.55	40.25
Outlet liquid temperature, T_{out}^{l} (°C)	53.35	51.95
Outlet CO_2 liquid loading	0.2802	0.2726
Outlet H_2Sliquid loading	0.2143	0.2143
CO_2 Outlet gas composition (PPM vol.)	8481.0	10,530.1
H_2S Outlet gas composition (PPM vol.)	4.8	9.2
Tower Diameter (cm)	149.4	149.4
# of Stages	18	26

Table III Effect of Tower Pressure on Sour gas Outlet Composition

		MEA		DEA	
P (bar)	D (cm)	$y_{CO_2,Out}$	$y_{H_2S,Out}$	$y_{CO_2,Out}$	$y_{H_2S,Out}$
10	180.1	0.1238E-1	0.6085E-5	0.3379E-1	0.3069E-4
20	163.3	0.5771E-2	0.2818E-5	0.2257E-1	0.1978E-4
30	157.9	0.2993E-2	0.1483E-5	0.1587E-1	0.1378E-4
40	156.7	0.1495E-2	0.7884E-6	0.1107E-1	0.9605E-4
50	157.6	0.6905E-3	0.4248E-6	0.7399E-2	0.6486E-5
60	159.7	0.2935E-3	0.2441E-6	0.4649E-2	0.4182E-5

Figure Captions:

Figure 1. a Schematic Diagram of the Film Model as Applied to a Tray in an Absorption Tower.

Figure 2. CO_2, H_2S, and DEA Concentration Profiles in the Liquid Film on the Fifth Stage.

Figure 3. CO_2 and H_2S Vapor Composition Profiles Versus Stage Number in the MEA Absorber.

Figure 4. CO_2 and H_2S Vapor Composition Profiles Versus Stage Number in the DEA Absorber.

Figure 5. CO_2 and H_2S Enhancement Factors Profiles Versus Stage Number in the DEA Absorber.

Figure 6. CO_2 and H_2S Liquid Loading Profiles Versus Stage Number in the DEA Absorber.

Figure 7. CO_2 and H_2S Efficiency Profiles Versus Stage Number in the DEA Absorber.

Figure 8. Temperature of the Gas Leaving a Stage Versus Stage Number in the DEA Absorber.

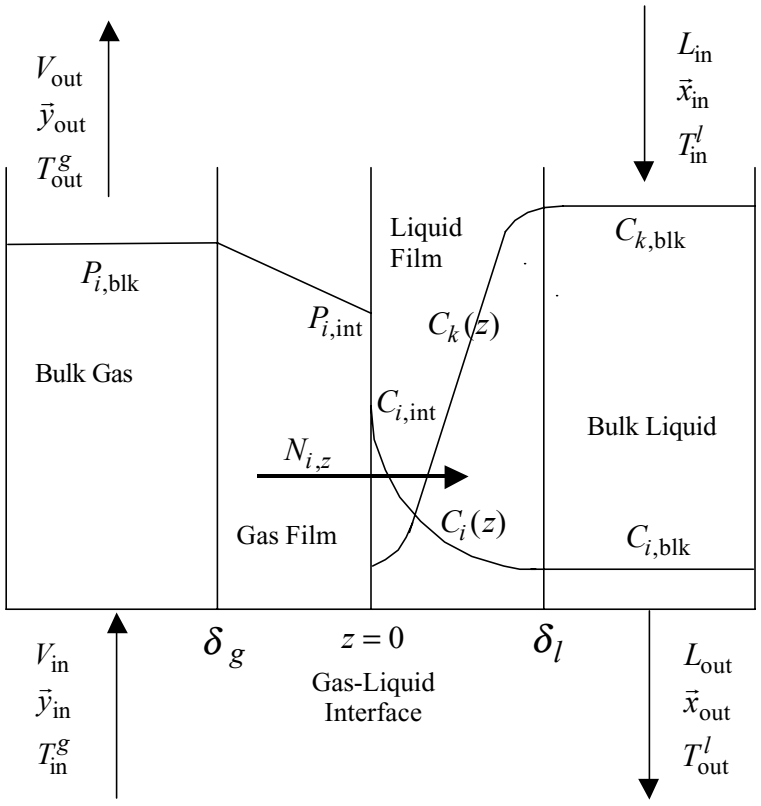
V_{out}
$\vec{y}_{\text{out}}$
T^g_{out}
L_{in}
$\vec{x}_{\text{in}}$
T^l_{in}
Liquid
Film
$C_{k,\text{blk}}$
$P_{i,\text{blk}}$
$P_{i,\text{int}}$
$C_k(z)$
Bulk Gas
$C_{i,\text{int}}$
Bulk Liquid
$N_{i,z}$
$C_i(z)$
Gas Film
$C_{i,\text{blk}}$
V_{in}
$\vec{y}_{\text{in}}$
T^g_{in}
δ_g
$z = 0$
Gas-Liquid
Interface
δ_l
L_{out}
$\vec{x}_{\text{out}}$
T^l_{out}

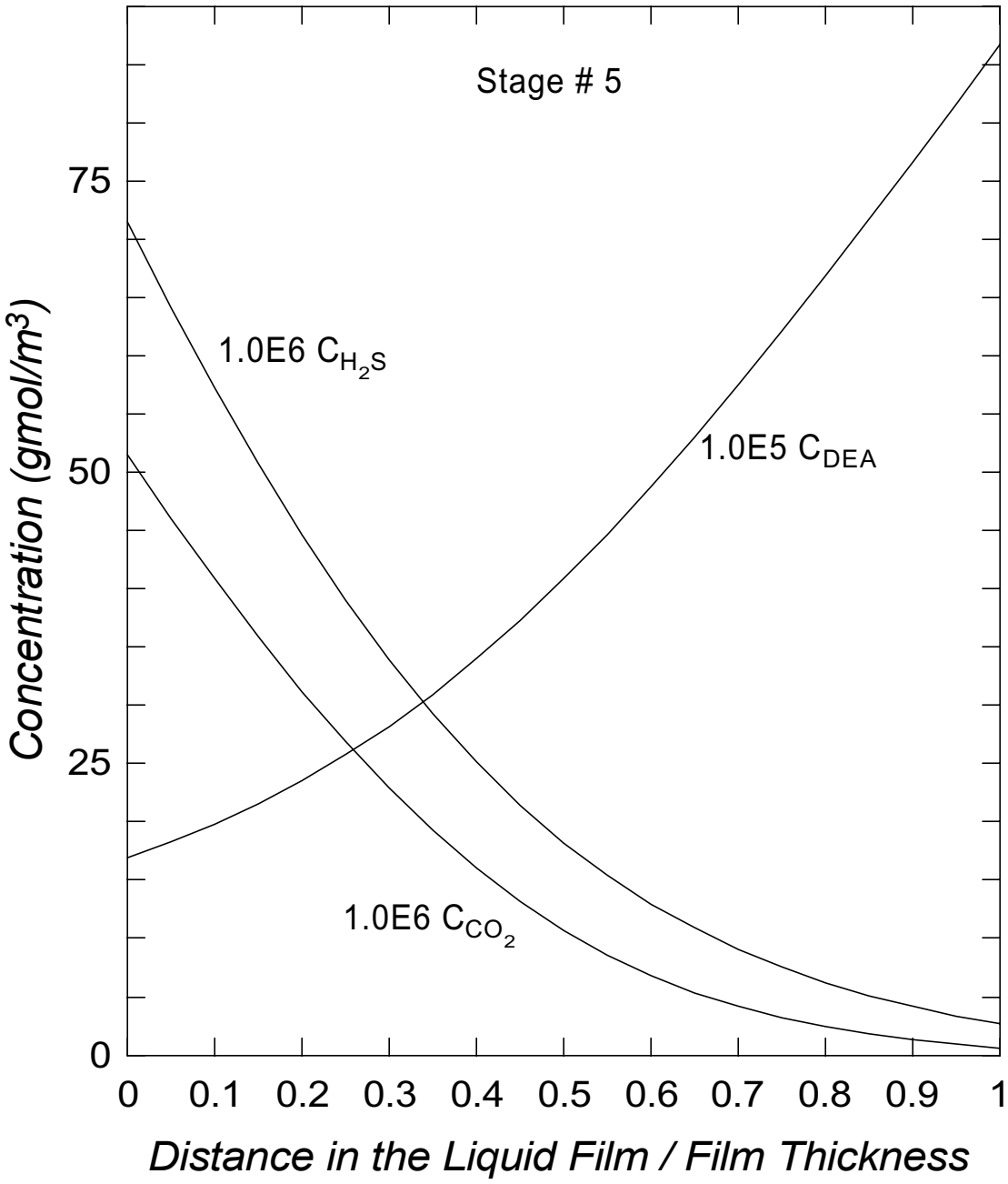
Stage # 5
75
50
25
0
Concentration (gmol/m3)
1.0E6 CH2S
1.0E5 CDEA
1.0E6 CCO2
0
0.1
0.2
0.3
0.4
0.5
0.6
0.7
0.8
0.9
1
Distance in the Liquid Film / Film Thickness

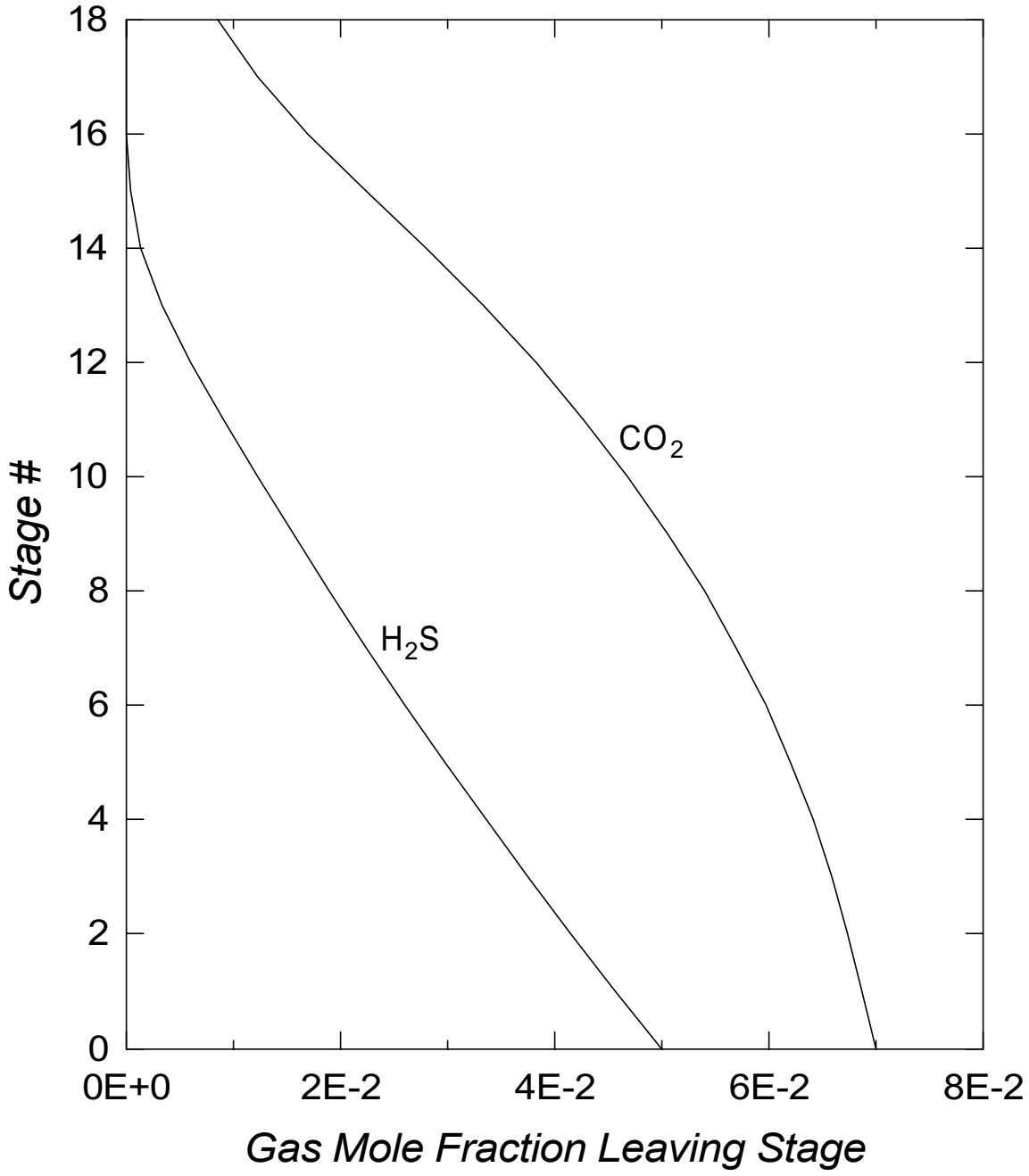
18
16
14
12
10
8
6
4
2
0
Stage #
CO2
H2S
0E+0
2E-2
4E-2
6E-2
8E-2
Gas Mole Fraction Leaving Stage

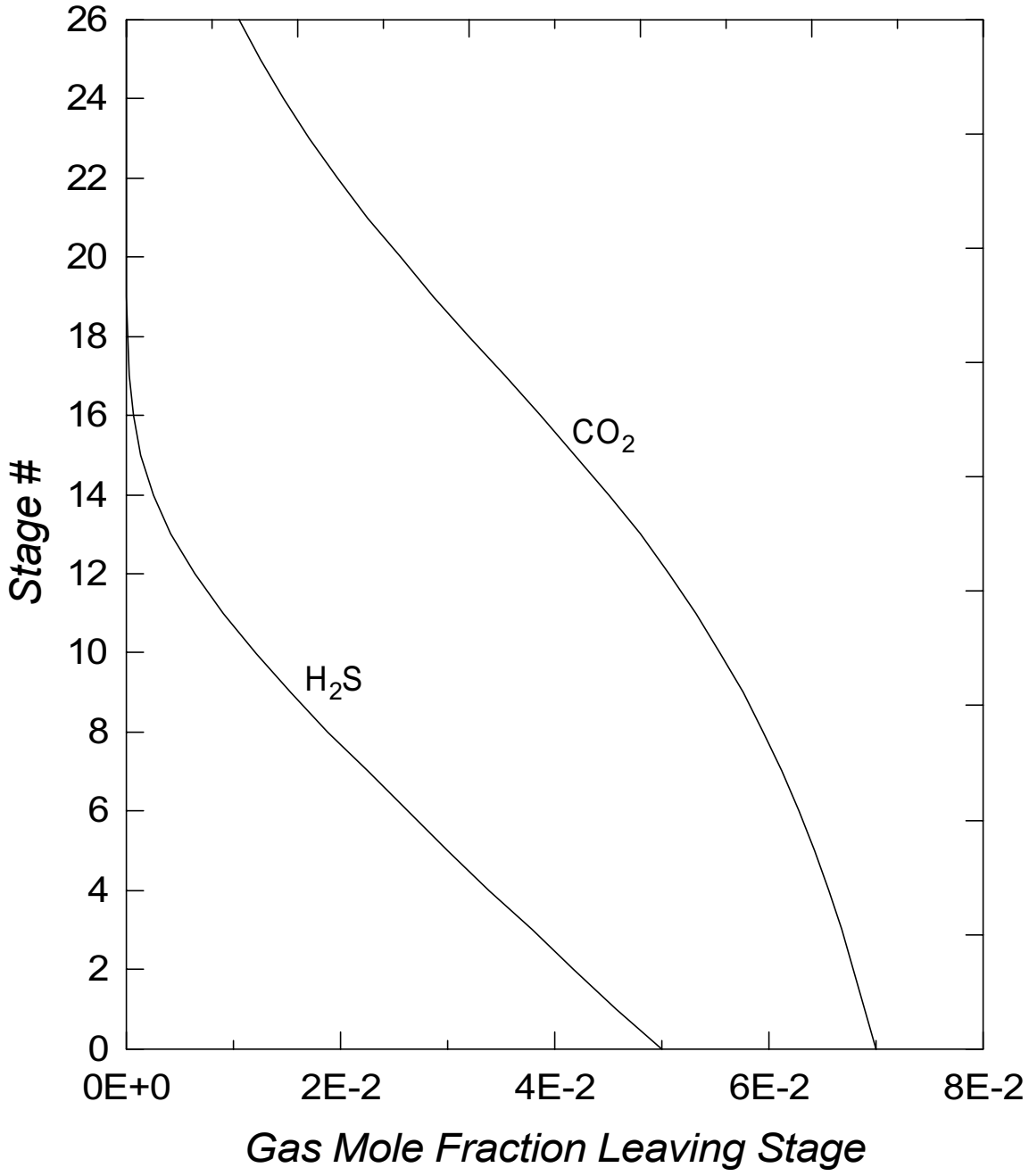
26
24
22
20
18
16
14
12
10
8
6
4
2
0
Stage #
CO2
H2S
0E+0
2E-2
4E-2
6E-2
8E-2
Gas Mole Fraction Leaving Stage

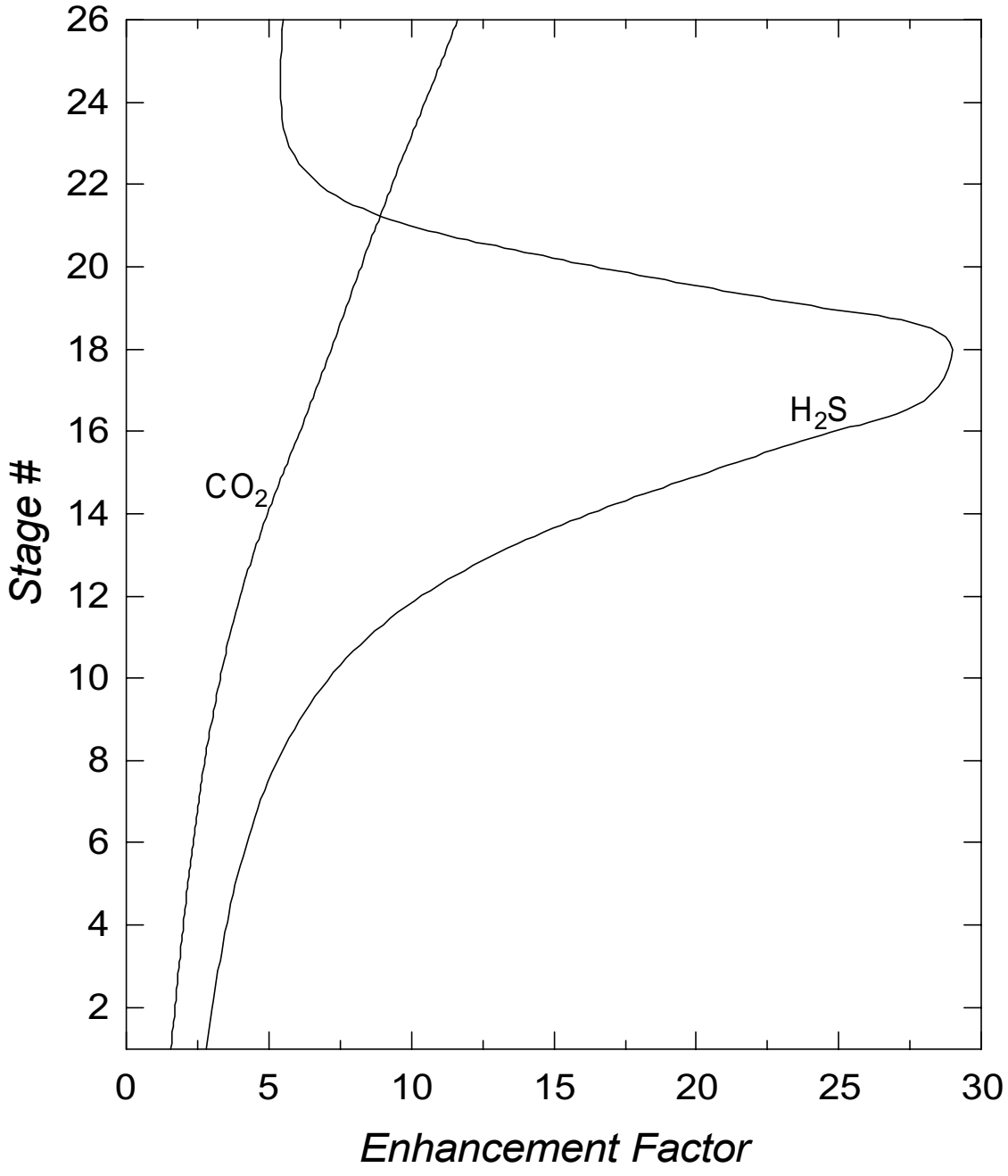
26
24
22
20
18
16
14
12
10
8
6
4
2
Stage #
0
5
10
15
20
25
30
Enhancement Factor
CO2
H2S

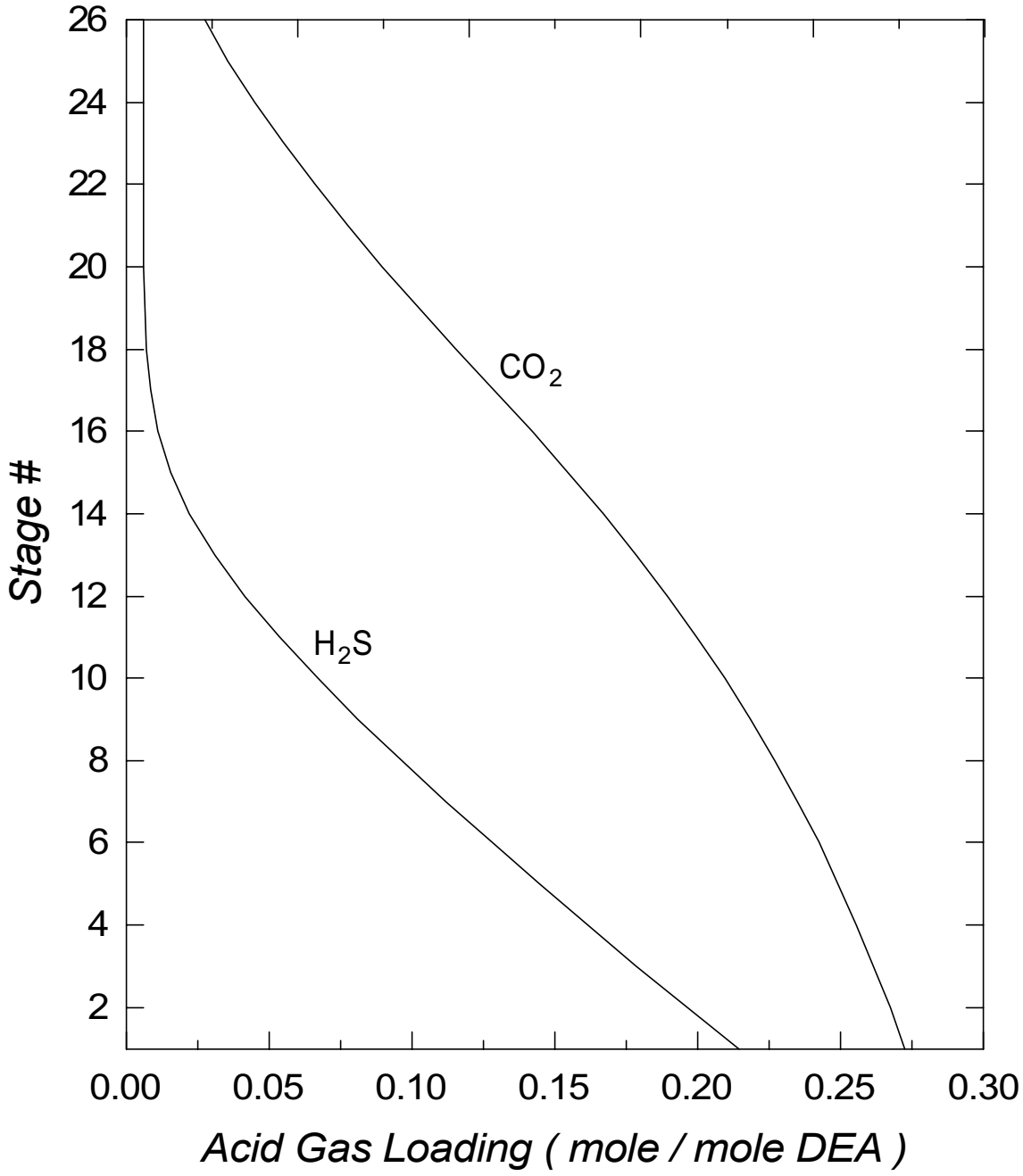
26
24
22
20
18
16
14
12
10
8
6
4
2
Stage #
CO2
H2S
0.00
0.05
0.10
0.15
0.20
0.25
0.30
Acid Gas Loading (mole / mole DEA)

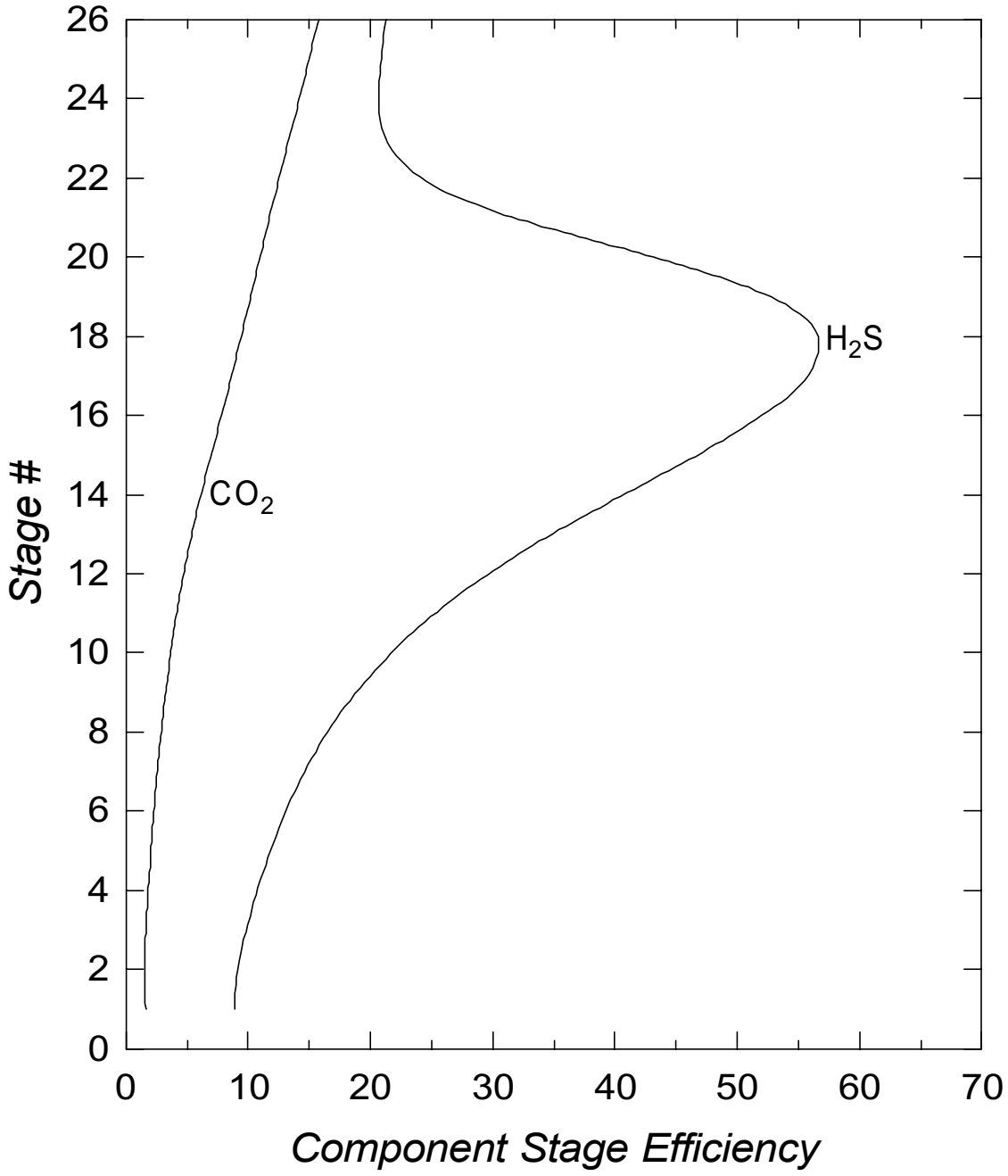
26
24
22
20
18
16
14
12
10
8
6
4
2
0
Stage #
0
10
20
30
40
50
60
70
Component Stage Efficiency
CO2
H2S

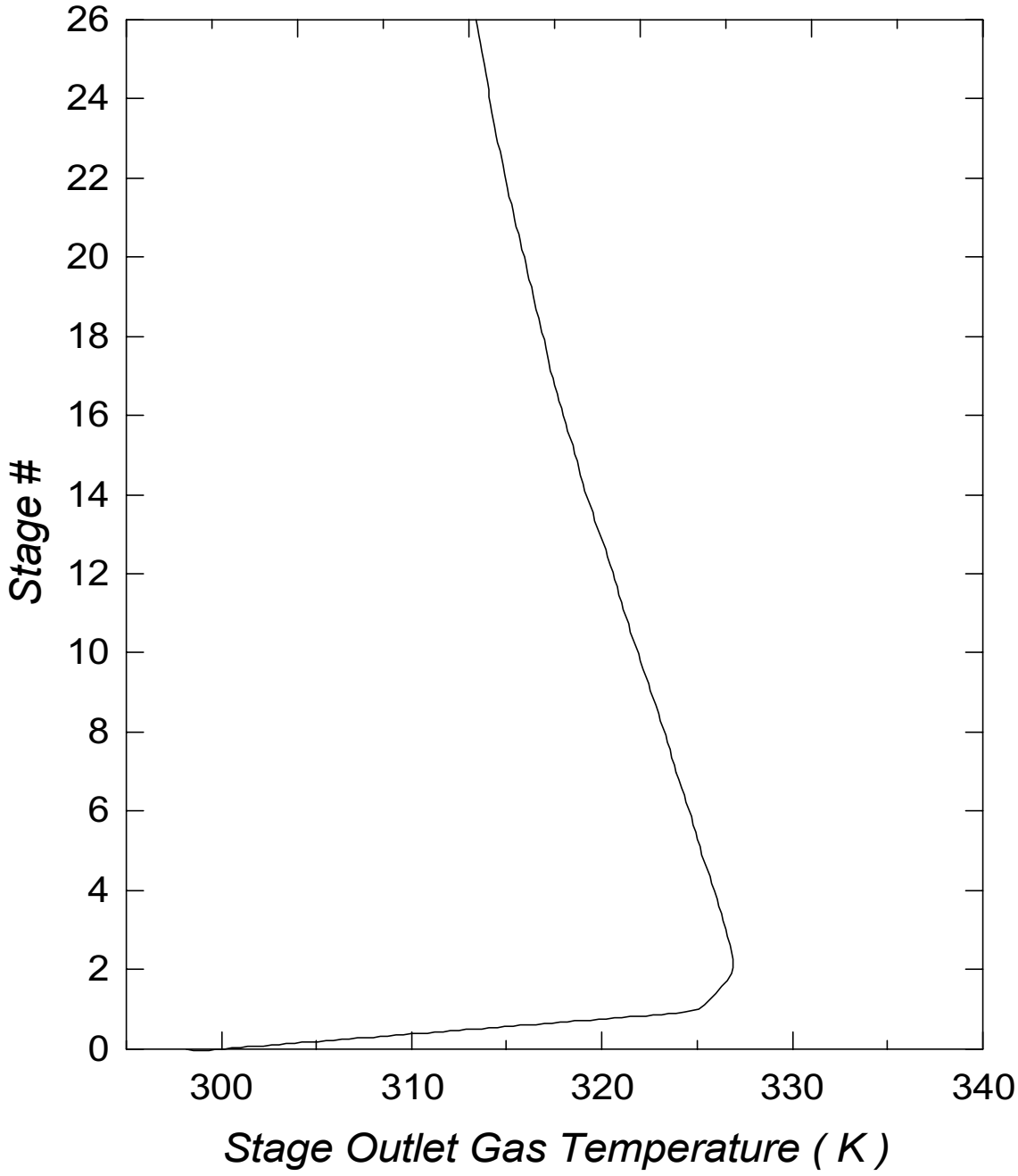
26
24
22
20
18
16
14
12
10
8
6
4
2
0
Stage #
300
310
320
330
340
Stage Outlet Gas Temperature (K)